Confocal Nanoscanning, Bead Picking (CONA): PickoScreen Microscopes for Automated and Quantitative Screening of One-Bead One-Compound Libraries

Martin Hintersteiner,[†,‡] Christof Buehler,[‡,§] Volker Uhl,[‡] Mario Schmied,[‡] Jürgen Müller,[||] Karsten Kottig,[||] and Manfred Auer*[,†,‡]

School of Biological Sciences (CSE) and School of Biomedical Sciences (CMVM), The University of Edinburgh, Michael Swann Building, 3.34, The King's Buildings, Mayfield Road, Edinburgh, EH9 3JR, U.K., Supercomputing Systems AG, Technoparkstrasse 1, CH-8005 Zürich, Switzerland, Innovative Screening Technologies Unit, Novartis Institutes for BioMedical Research (NIBR), Brunnerstrasse 59, A-1235 Vienna, Austria, and PerkinElmer Cellular Technologies Germany GmbH, Schnackenburgallee 114, 22525 Hamburg, Germany

Received April 13, 2009

Solid phase combinatorial chemistry provides fast and cost-effective access to large bead based libraries with compound numbers easily exceeding tens of thousands of compounds. Incubating one-bead one-compound library beads with fluorescently labeled target proteins and identifying and isolating the beads which contain a bound target protein, potentially represents one of the most powerful generic primary high throughput screening formats. On-bead screening (OBS) based on this detection principle can be carried out with limited automation. Often hit bead detection, i.e. recognizing beads with a fluorescently labeled protein bound to the compound on the bead, relies on eye-inspection under a wide-field microscope. Using low resolution detection techniques, the identification of hit beads and their ranking is limited by a low fluorescence signal intensity and varying levels of the library beads' autofluorescence. To exploit the full potential of an OBS process, reliable methods for both automated quantitative detection of hit beads and their subsequent isolation are needed. In a joint collaborative effort with Evotec Technologies (now PerkinElmer Cellular Technologies Germany GmbH), we have built two confocal bead scanner and picker platforms PS02 and a high-speed variant PS04 dedicated to automated high resolution OBS. The PS0X instruments combine fully automated confocal large area scanning of a bead monolayer at the bottom of standard MTP plates with semiautomated isolation of individual hit beads via hydraulic-driven picker capillaries. The quantification of fluorescence intensities with high spatial resolution in the equatorial plane of each bead allows for a reliable discrimination between entirely bright autofluorescent beads and real hit beads which exhibit an increased fluorescence signal at the outer few micrometers of the bead. The achieved screening speed of up to 200 000 bead assayed in less than 7 h and the picking time of ~1 bead/min allow exploitation of one-bead one-compound libraries with high sensitivity, accuracy, and speed.

Introduction

Screening of large compound collections for biologically active molecules is the predominant initial step in drug discovery. Random screening resembles the proverbial search for the needle in a haystack.[1] Usually, hundreds of thousands of molecules are screened with initial hit rates around 0.1%, i.e. one hit is found in 1000 compounds. After elimination of false positives, the actual number of valuable compounds derived from such screening campaigns is even smaller. Substantial investments into miniaturization and automation have made high throughput screening (HTS) in solution a faster more efficient and more reliable process. Irrespective of technical improvements, traditional HTS depends on large compound archives.[2] However, large compound collections are only accessible to big pharmaceutical companies. They require considerable resources for generating and maintaining a stock of compounds, the majority of which turn out to be inactive.[3] Therefore, on-bead screening (OBS), i.e. the identification of ligands from large one-bead one-compound (OBOC) combinatorial libraries, has been developed as an alternative screening method that is not dependent on costly compound archives.[4−11] After three decades of development, solid phase combinatorial chemistry allows generating large bead based libraries. These can easily contain hundreds of thousands to millions of compounds prepared at very low costs compared to standard library synthesis which involves extensive compound purification. The accessibility of large OBOC libraries together with a generic, fast, and resource efficient method for testing the primary binding affinity of a

* Corresponding author. E-mail: manfred.auer@ed.ac.uk. Office phone: +441316505346.
[†] The University of Edinburgh.
[‡] Novartis Institutes for BioMedical Research (NIBR).
[§] Supercomputing Systems AG.
[||] PerkinElmer Cellular Technologies Germany GmbH.

10.1021/cc900059q CCC: $40.75
Published on Web 07/15/2009

substance at the site of its synthesis are the essential advantages of on-bead screening.

In OBS, hits are identified by detecting the binding of a target protein to ligands immobilized on ~100 μm sized resin beads. Various different methods for visualizing this protein−ligand complex formation on the bead surface have been described in the literature,[12−16] including the use of fluorescently labeled proteins, fluorescently labeled antibodies for secondary detection, and radiolabeling or enzyme linked colorimetric assays, to name but a few. In this paper, we particularly focus on using fluorescently labeled target protein and fluorescence based confocal microscopy detection for hit bead identification. Identified hit beads are then isolated to determine the compound structure via mass spectrometry[17,18] or other decoding methods.[19−21]

Therefore, an OBS process involves detecting, quantifying, ranking, and isolating a small number of fluorescent hit beads (usually the best 10−100) from a large stock of library beads (≈10 000−1 000 000 beads). Although standard fluorescence microscopes have been used for hit bead detection, these approaches generally suffer from low signal-to-noise ratios due to varying levels of autofluorescence.[13,22,23] In addition, the manual isolation of hit beads is slow and often tedious. As autofluorescence is associated with the entire bead volume, the background signal can easily be higher than the fluorescence associated with target protein binding to compounds on the bead's surface.

To date, the complex objects and particle sorter (COPAS, Union Biometrica, MA) represents the only commercially available OBS instrument. On the basis of fluorescence activated bead-sorting, COPAS allows analyzing and sorting of libraries at a speed of up to 20 beads/s.[24] However, the instrument is operated in an attended mode, and the need for pausing and constantly refilling the sample compartment limits the effective screening throughput to about 50 000−150 000 beads/day. As analysis and sorting is performed on the fly, establishing appropriate gate settings for retrieving the best hits can be problematic. In addition, reliable screening of hit beads on COPAS is only possible if the libraries are presorted to remove beads with high levels of autofluorescence.[23,25]

To address these issues, we have developed the first automated on-bead screening platform "PickoScreen" for automated confocal nanoscanning and bead picking (CONA). The instruments, which we describe herein, have a primary screening capacity of up to 200 000 beads/day and incorporate high-speed automated confocal bead scanning, efficient image segmentation algorithms (quantitative bead detection), hit bead selection parameters, and an automated hit bead isolation procedure, called bead picking.

Instrumental Requirements

TentaGel (TG) beads of 90 μm diameter are the most popular resin type for on-bead screening due to their excellent swelling properties in water and superior mechanical stability. The beads are microporous and consist of a polystyrene core onto which polyethyleneglycole (PEG) is grafted to a final content of 50 to 70% (w/w).[26] The narrow pore size of TentaGel resins typically prevents fluorescently labeled target proteins, usually larger than 15 kDa, from penetrating into the bead interior within the typical incubation and screening time. This confines the majority of the relevant signal to the bead periphery, i.e. the volume encompassing the outer few micrometers of the bead. In addition, the microenvironment at the outside of a TG bead provides the closet possible match to a physiological buffer screening environment. We therefore hypothesized that a confocal detection system with its 3D-confined small detection volume ($\leq 10^{-15}$ L) is needed to measure protein binding at the bead periphery with micrometer optical resolution, high accuracy, and sensitivity. Standard confocal microscopes incorporate single-beam laser scanning optics which results in low frame rates (s) and small fields of view (a few hundred micrometers). Due to the relatively large bead diameter in the swollen state, of approximately 100 μm, both large area scanning and parallel (confocal) detection schemes are prerequisites to achieve an adequate sample throughput rate on the order of 200 000 beads/day. A monolayer of beads on the glass bottom of one well of a 96-well microtiter plate (MTP) comprises about 2000 beads ($\varnothing \approx 100$ μm), this amounts to a total of about 200 000 beads per plate. Thus, the design and implementation of a high-speed confocal on-bead screening platform capable of automated scanning of an entire 96-well MTP and capable of isolating the detected hit beads in less than a day represents a specific engineering challenge. The key requirements of such a scanning/picking microscope for screening bead based combinatorial compound libraries are summarized below:

Confocal Optics. For on-bead screening, a monolayer of beads placed on the bottom of an MPT is incubated with a low nanomolar concentration of fluorescently labeled target protein. Thus, the screening protein solution generates a low background fluorescence comparable to typical fluorescence fluctuation analyses at single molecule resolution. 3D-Confined confocal imaging can effectively discriminate the fluorescence background against the fluorescence signal derived from the bead-bound protein.

Resolution and Quantification. Within the time of an on-bead screen, the association of the labeled target protein to the compound linked on the bead is limited to the outermost section of a bead, which becomes manifest in a sharp fluorescent "ring" in the confocal scan image. Further, the scan images must also be acquired with both high mechanical precision (micrometer-scale) and detection accuracy to allow for reliable automated data acquisition and quantification of the fluorescence intensities within the "rings".

Automation and Speed. Combinatorial on-bead libraries may comprise several thousand to hundreds of thousands of compounds. In order to build an efficient screening process, a full library must be screenable in an automated fashion within a few days. Semiautomated operation for hit bead isolation is acceptable for the expected hit rates of ~0.1% and taking into account that only the "best" hit beads, i.e. beads with the highest fluorescence ring intensity, are to be picked (cherry picking).

In a joint collaborative effort with Evotec Biosystems and further on Evotec Technologies (now Perkin-Elmer), we have developed and implemented two confocal bead scanner and

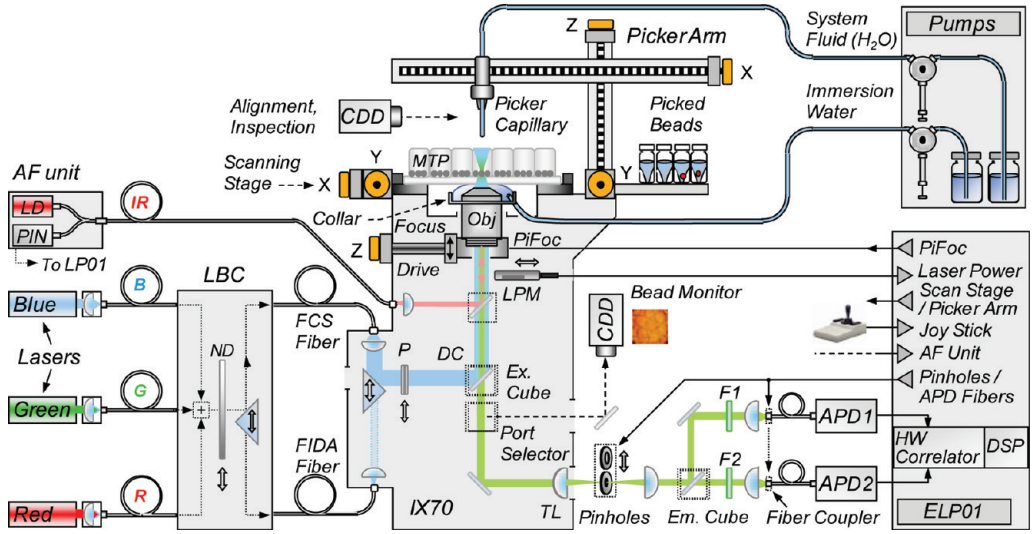

Figure 1. Schematic diagram of the confocal bead scanner and picker instrument PS02. PS02 functionalities encompass confocal large area scanning of microtiter plates, bead detection, quantification, and ranking and picking of ranked hit beads. Three different laser sources can be superimposed via a laser beam combiner (LBC), fiber-coupled into a modified inverted microscope (IX70, Olympus). The laser power is set by means of a neutral density (ND) filter slider. The optical port selector (⇔) routes the emission light path either to the binoculars (not shown), the confocal detection optics (APDs), or the CCD video camera for macroscopic bead monitoring. Confocal bead scanning is accomplished via a stepper-motor-driven *x*/*y* stage. The scanning height (*z*-axis) is set via both the focus drive and the piezo-driven objective translator (PiFoc). Automatic finding and adjustment of the scanning height is accomplished via the autofocus (AF) unit with integrated infrared laser diode (LD) and PIN photodiode. They are jointly coupled into the excitation light path by a common single-mode fiber (*y* splice). The glass bottom of the sample carrier reflects the auxiliary laser light back into the autofocus unit. Due to the confocal-like setup of the *y*-spliced fiber, the backreflected intensity depends on the actual *z* position of the sample carrier. The fluorescence emission components are transmitted through bandpass filters (F1, F2), coupled into optical fibers with DC-motorized couplers, and detected by fiber-coupled single-photon sensitive avalanche photodiodes (APDs). The APD output signals are routed to the CTRL-BOX (EBL01, Evotec, Germany) with integrated hardware correlator board for rapid Single Molecule Detection (SMD) analysis (not used in bead scanning mode). In addition, the CTRL-BOX incorporates driver cards (right-pointing triangle symbols) for the various modules (e.g., the stepper motors ⊙) and a digital signal processor (DSP) board which adjusts the user-requested scanning height via a feedback loop involving the AF and PiFoc units and communicates with the host computer (not shown here). Bead picking is accomplished via a small capillary which is mounted and connected to a computer-controlled robotic arm and a hydraulic system, respectively. A custom-designed objective collar with hydraulic-driven liquid supply ensures appropriate resupply of immersion water in case of extended scan times. Abbreviations: APD = avalanche photo diode, CCD = charged coupled device, DC = dichroic mirror, DSP = digital signal processor, ELP01 = Evotec control box, F = filters, IR = infrared, IX70 = inverted microscope from Olympus, HW = hardware, MTP = microtiter plate, LPM = laser power meter, ND = neutral density filter, P = polarizer, R/G/B = red/green/blue, BPS = polarizing beam splitter, TL = tube lens, PBS = polarizing beam splitter.

picker platforms, i.e. PS02 and its high-speed variant PS04, that address the above listed requirements.

Materials and Methods: Instrument Description

Confocal Bead Scanner/Picker Platform PS02. The PS02 instrument is based on an Olympus IX70 inverted microscope and Evotec's FCS+plus Research Reader (Figure 1; for photographs of key components, see Figure S1 of the Supporting Information). PS02 further incorporates (1) three fiber-coupled laser sources for fluorescence excitation in the visible wavelength range, (2) a laser beam combiner (LBC) for multicolor illumination, (3) a neutral density (ND) filter slider and laser power meter (LPM) for laser power measurements and adjustments, (4) two selectable confocal pinholes (50 and 70 μm), (5) a dual-channel detection scheme with single-photon sensitive avalanche photodiodes (APDs), (6) an autofocus unit (AF), (7) a stepper-motor-driven *x*/*y* scanning stage, (8) an automated immersion water supply, (9) a computer controlled robotic arm with hydraulic-driven capillary for isolating (picking) identified beads, and (10) Evotec's proprietary software for instrumental control and data analysis. For a detailed description of PS02 "standard components" as a confocal MTP reader for fluorescence fluctuation analysis, see the Supporting Information.

Bead Scanning Process. Typically, a 96-well glass bottom MTP (e.g., from Greiner) is used as sample carrier for on-bead screening. The glass bottom thickness is 170 μm. Each well contains a monolayer of approximately 2000 beads (100 μm diameter). The MTP is screened by linewise scanning the full area of each well at a constant focus height. The actual scan height above each well bottom is automatically determined and adjusted by means of the autofocus unit, the piezo-driven objective translator, and the EVOcorr DSP board (Figure 1). The AF unit comprises a diode laser (wavelength 780 nm, power 3 mW) and a silicon Positive Intrinsic Negative (PIN) photodiode with a photocurrent-to-voltage amplifier (P-9202, Gigahertz Optik). The laser light and the PIN diode are combined by a *y*-spliced single-mode fiber (Gould 50:50 splitter). The fiber ends coupled into the PS02 excitation light path such that the small fiber core forms a confocal pinhole. By translating the objective along the *z*-axis, the PIN diode detects two intensity peaks that correspond to the lower and upper surface of the MTP glass bottom. The EVOcorr DSP board records the intensity trace

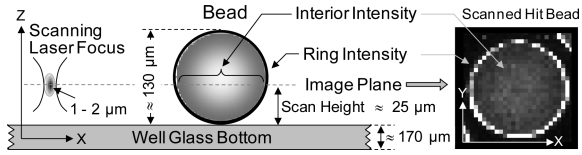

Figure 2. Confocal bead scanning parameters. (left) Schematic illustration of laser focus, its actual scan height through the beads (image plane), and the two fluorescence analysis zones: "interior intensity" and "ring intensity". The interior intensity is the average fluorescence intensity within the refractive index dependent confocal focus extension in the *z*-direction throughout the bead interior. The ring intensity is the average fluorescence intensity detected from the confocal focus extension in the *z*-direction in the outer 5 μm of the bead (= ring). (The depicted dimensions do not scale.) (right) Representative fluorescence image of a hit bead.

and transmits it to the control PC, which implements the autofocus procedure including the peak fitting algorithm. In practice, the actual scan height is set to about 25 μm above the MTP glass bottom, thus intersecting the beads slightly below their equatorial plane.

Bead scanning is accomplished by linewise translating the sample carrier via a stepper-motor-driven *x*/*y* scan table (Märzhäuser, Wetzlar/Germany). The mechanical positioning resolution is better than 1 μm. Pixel based images are constructed by binning the detected photons of each line into consecutive time intervals. Thus, the image resolution is determined by the optical resolution of the confocal point-spread function, the scan speed, and the binning scheme of the photon arrival times into consecutive image pixels.

The software allows control of the scan speed and hence the lateral resolution. In a typical screening situation, the lateral resolution per pixel was set to 5 μm (scan speed = 8 mm/s, bin time = 70 μs). These settings provide maximal speed at moderate resolution and are adequate for most screening situations (see below). Using these settings, for a full 96-well MTP the resulting total scan time is 72 h. The relevant scan and bead analysis parameters are shown in Figure 2.

Bead Localization Algorithm and Ranking. After all scan images are recorded, they are analyzed to identify, localize, and quantify the beads using geometrical and fluorescence parameters including size and brightness distribution. The quantitative image information is used to classify the beads and to generate a prioritized bead retrieval list.

The bead localization algorithm includes individual processes to perform (1) an optional noise reduction and contrast compression step (5 × 5 pixel averaging and logarithmic scaling, user selectable), (2) an edge enhancement via a Sobel operator,[27] and (3) a thresholding algorithm controlled by a user-defined threshold which generates a binary mask of the bead edge pixels.

A generalized Hough transformation[28] is then applied to the binary mask image to identify objects of approximately circular shape. This identification step is parametrized by a target bead size and a user-supplied tolerance parameter. Center coordinates and radii of each identified bead are provided as the output.

Next, the spatial distribution of fluorescence intensity is assessed for each bead, by reverting to the original intensity image and by applying the previously determined position and radius information. Two output parameters are provided for each bead: (a) an "interior intensity", averaged over the full circular cross-section captured in the scan and (b) a "ring intensity", averaged over a narrow ring (of user-selected width) along the perimeter of the bead.

Bead Picking Process. The PS02 bead picker unit consists of a robotic arm with a mounted bead-picking capillary. The picker capillary, made from polyimide tubing (for standard 90 μm TG beads 142 μm inner diameter, HV Technologies, Trenton, GA) is glued into a small solder paste dispenser support. The capillary is mounted via its luer lock on the robotic arm and connected to the hydraulic system.

The picker robotics can exploit an extended 3D translation range with micrometer resolution including the scan table and the bead deposition site. Each translation axis comprises a precision linear stage with a travel range of a maximum of 150 mm (MICOS PM90). Driven by stepper-motors, the maximal translation speed of each stage is 20 mm/s. Successful bead picking requires calibration of the scan table and picker capillary coordinates. Course position calibration is achieved via end-switch based table homing and joy-stick-driven alignment of the capillary tip using a visual reference point and a video-rate camera (Figure 1, alignment/inspection CCD). The final calibration particularly in the *z*-direction is achieved by manually positioning the capillary tip right above the well bottom area located right above the microscope objective, i.e. in the center of the field of view. Both the beads and the capillary tip are observable via a video-rate camera that is attached to a side port of the microscope (Figure 1, bead monitor, KamPRO 04, EHD, Damme/Germany). Wide-field illumination is provided by a ring-shaped fiber-coupled cold light source (PS02: Illumination Technologies Inc. 3900. PS04: Linus LQ1100) that surrounds the picker capillary.

The bead retrieval process is performed semiautomatically. Typically, the wells comprising hit beads are identified in a preceding full-plate scan. For each well of interest, the beads are rescanned to cope with potential dislocation artifacts. The center positions of the beads are identified by the Hough transformation algorithm as described above, their surface and ring intensities are derived, and—depending on user-defined threshold criteria—a prioritized pick list is generated. Then, the picker robotics semiautomatically retrieves each bead from the pick list, one-by-one, by moving the picker capillary right above a bead until it is fully engulfed by the tip opening, applying hydraulic pressure to absorb the bead into the capillary tip, gently lift the tip out of the well, and eject the captured bead into a an appropriate container (e.g., MTP, of MS-vial). Scanning and bead picking requires liquid handling steps: (a) replacing the immersion water of the objective on a well-per-well basis (≈5 mL reservoir); (b) aspirating, depositing, and rinsing HPLC grade water of the picker needle. This process consumes ≤20 μL per bead. All hydraulic components are driven by computer-controlled Kloehn syringe pumps (Model 50400, Kloehn Inc., Las Vegas, NV).

Nipkow-Based Scanner/Picker Platform PS04. PS02 provides high resolution and high sensitivity detection of the library beads at moderate sample throughput. For achieving

Table 1. Instrumental key parameters for PS02 and PS04. The listed parameters for scan speed per well and per 96-well MTP are dependent on the chosen lateral resolution on PS02, set usually to 5 μm. The line scan speed at 5 μm resolution on PS02 is 8 mm/s. The exposure time of the PS04 cameras is 200 ms per tile image. The axial resolution of both PS02 and PS04 is $\leq 1\mu$m (confocal setup)

	scan speed		resolution	bead picker		data size	
	per well	per plate	lateral: *x*/*y*	calibration	picking	per well	per plate
PS02	45 min	72 h	5 μm	15 min	$\approx$180 s/bead	$\approx$3 MB	$\approx$288 MB
PS04	5 min	7 h	1 μm	15 min	$\approx$70 s/bead	$\approx$12 MB	1.17 GB

HTS performance, PS04 was equipped with a high-speed spinning disk, "Nipkow-Technology".[29−31] The basic instrumental layout of PS04 including lasers, the microscope (IX70 with UApo 40x objective, Olympus), and picker robotics is identical to PS02. Attached to the right side port of the microscope, the Nipkow disk scanner (CSU10, Yokogawa, Japan) incorporates about 20 000 pinholes and microlenses (exact number not disclosed by Yokogawa) and achieves scan speeds of up to 360 frames/s. The individual pinhole diameter is 50 μm. The CSU10 module provides a fiber-coupled excitation light channel and two detection channels with spectral separation between 495−535 nm (channel1: 515/40) and 665−715 nm (channel2: 690/50). For each detection channel, the image is captured by a cooled 12-bit CCD camera (SensiCam QE, PCO, Kelheim, Germany). The excitation light at 488 and 633 nm is generated by two laser sources: a 200 mW optically pumped semiconductor laser (Sapphire 488-200 CDRH, Coherent) and two combined 22 mW (each) Coherent helium−neon lasers, respectively.

Analogous to the PS02, appropriate experimental settings were determined in test experiments by balancing scan speed versus image quality. As for PS02, the confocal scan height was 25 μm (Figure 2). 96-well glass bottom MTPs (170 μm glass thickness) were used as sample carriers. Because the image size of a single Nipkow scan is much smaller than the well size, full-well images are generated by automatically moving the sample stage to adjacent subregions and merging the correspondingly recorded series of tile images. For a camera exposure time of 200 ms per tile image and a 8 × 8 pixel binning scheme, a spatial overlap of 30% between adjacent tile images provides satisfying image quality and results in 823 tile images per well. The total scan time of a 96-well standard MTP, i.e. about 200 000 beads, is <7 h.

The background signal and the nonuniformity of the illumination field are corrected via the acquisition of a dark image (laser shutters closed) and a reference image (plain dye solution), respectively. Due to the excessive computational time required ($\approx$5 min/well), the image merging procedure is performed on a separate computer. A switch-based GigaBit LAN connection to PS04 allows executing the merging algorithm during the image acquisition of the next well. Only merged images are stored using the LuraWave compression algorithm (LuraTech Europe, Berlin/Germany). Typical data volumes are listed in Table 1.

Typical Assay Conditions for CONA on-Bead Screening. For CONA on-bead screening, the target proteins are most often labeled with fluorescent dyes by e.g. random labeling of lysines or cysteins using commercially available *N*-hydroxysuccinimidyl ester or maleimido functionalized fluorophores, e.g. from Invitrogen, and following the manufacturer's protocol.

In a typical screening experiment, the wells of a 96-well microtiter plate with glass bottom are each filled with 1 mg of combinatorial library beads (TentaGel S, 90 μm from Rapp Polymers, Tübingen, Germany) and the beads are preblocked for 1 h, using buffers containing either BSA, gelatin, or a crude cell-lysate as blocking agents. The beads are then incubated with the buffer containing 5 to 50 nM of the fluorescently labeled target protein for several hours. After this incubation period, the plate is placed on the scanning table of the screening instrument and the CONA procedure, outlined above, is started. For screening on the PS02 instrument usually small sections, e.g. 2 × 2 mm from a few wells are recorded to optimally tune the signal intensities by adjusting the Optical Density (OD) filter in the excitation path.

Results

Scanning Speed, Image Resolution. To compare the basic performance parameters of PS02 and PS04, image resolution, scanning and picking speed, and data volume were measured, for each instrument, respectively (Table 1).

In a typical confocal optical setup (40× objective, NA = 1.25, 488 nm light), the lateral and axial resolution is about 0.2 and 0.8 μm, respectively.[32] The interaction zone of a target protein and a bead immobilized compound is confined to the outer 2−5 μm of a bead. At maximal resolution (pixel size $\leq$0.2 μm), this ring zone would encompass a surplus of data points. Thus, without compromising the reliable detection and quantitative assessment of hit beads, the optical resolution can be traded off against scan speed and data volume.

The image resolution on PS02 is determined by the scanning speed in the *x* dimension and by the number of lines in the *y* dimension. The scan speed is adjustable, but typically in the millimeters per second range. The sampling rate is 140 Hz at a constant photon bin time of 70 μs. To determine the optimal scan speed while maintaining the necessary resolution for a reliable detection of hit beads, bead images at different resolutions (5 and 10 μm) and hence different scan speeds/number of lines were recorded on the PS02 (Figure 3a). Whereas up to 10 μm resolution fluorescence ring intensity due to target protein binding can be distinguished from the interior intensity, a 10 μm resolution is clearly not sufficient for hit bead detection. For a refined assessment, the fluorescence profiles of a hit bead were analyzed at resolutions from 5 to 10 μm in 1 μm steps (Figure 3b). The final screening time per 96-well plate is not linearly dependent on the scan speed but also includes the time for

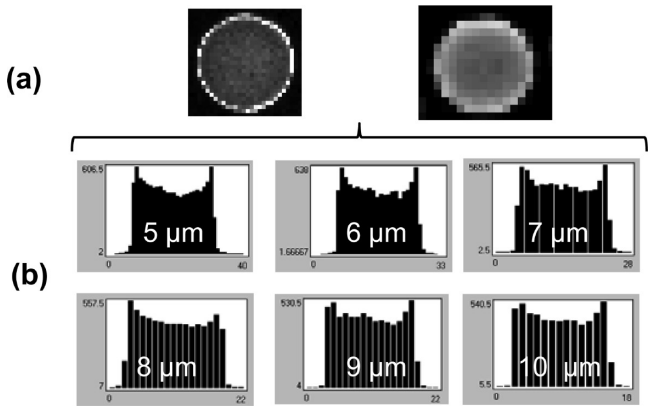

Figure 3. Image quality and bead profiles. (a) Hit beads imaged on PS02 at 5 and 10 μm lateral resolution. (b) Bead intensity profiles detected in a resolution of 1 μm steps, increasing from 5 μm (panel b, upper row, left) to 10 μm (panel b, lower row, right).

autofocus adjustment and for well to well propagation. (Figure S3 of the Supporting Information). In sum, this analysis revealed that a resolution of 5 μm still allows reliably detecting and ranking hit beads. It was therefore chosen as the default resolution parameter. The resulting screening time on PS02 is 45 min/well, or 72 h per 96-well MTP. With ~200 000 beads per MTP this equals a screening speed of 1.3 s/compound.

The bead screening time on PS04 is determined by the speed of the motor-driven sample stage (tile-to-tile, well-to-well), the image overlay factor, and the CCD exposure time (typically hundreds of milliseconds). The scan speed of the sample stage including its acceleration and retardation phase was adjusted to avoid potential disturbances of the bead monolayer. Further, the image overlap factor and the binning scheme of adjacent pixels on the CCD camera chip were optimized. Both parameters affect the resolution and data volume. In standard on-bead screens, good merging results were achieved with 25% overlap between adjacent tile images. This requires ≈760 tile images per well (96-MTP) for its full coverage. Adequate image contrast was achieved by binning 8 × 8 pixels. This setting corresponds to a lateral resolution of about 1 μm and leads to a data reduction by a factor of 64. Although the lateral resolution of PS04 is better than that of PS02, the contrast and sharpness of PS04 images are reduced primarily due to different background levels of APD vs CCD detectors, different dynamic ranges, and the need for image merging on PS04.

On-Bead Screening and Detection of Hit Beads. For a typical on-bead screening experiment on the PS0X instruments, ~1 mg of TentaGel beads from one-bead one-compound libraries are filled into each well of a 96-well MTP and incubated with a 5−50 nM concentration of a fluorescently labeled target protein. After a project dependent incubation period of usually several hours, the MTP containing the beads is agitated vigorously. Then, the rotating movement is stopped abruptly. This causes the reproducible formation of a bead monolayer at the bottom of each well.

To test the performance of both PS0X instruments in a real screening situation, test-screens with 50 nM of a Cy5 labeled target protein were performed. Representative images of whole 96-well MTP wells, recorded on PS02 and PS04 are displayed in Figure 4.

Using the parameters derived as described above, the achieved image quality readily allows discriminating individual beads against their neighbors and interbead background on both instruments. Bead sizes appear remarkably uniform with some minor variations due to the manufacturing process. The majority of beads exhibit only background fluorescence without any enhancement at their periphery (ring). The intrabead fluorescence however varies significantly, ranging from virtually none (dark spots) to excessive levels (Figure 4, left insert). Such bright beads not only give rise to false positives in nonconfocal detection methods but could potentially damage the APDs in the confocal setup of the PS02. Therefore, PS02 includes a software based intensity threshold above which the APD is turned off automatically for several seconds while scanning continues (Figure S4 of the Supporting Information). Screening samples regularly contain fragmented beads. Damaged beads are excluded in the bead analysis algorithm by discarding objects with a significant deviation from an ideal circle. As demonstrated in Figure 4, both instruments, PS02 and PS04, can reliably discriminate between hit beads with bound fluorescent target, beads exhibiting only background fluorescence, and autofluorescent beads. Hit beads display an increased fluorescence intensity on the bead edges (called increased fluorescent ring intensity) compared to the fluorescence intensity in the beads' interior. Typical values for fluorescence ring intensities over background intensity are 10− 50× for PS04 and 10−500× for PS02. As outlined above, PS04 recorded images exhibit a reduced image quality although the nominal optical resolution of PS04 (1 μm) is higher than that of PS02 (5 μm) under standard settings. Nevertheless, the sharpness and contrast of PS04 images are sufficient for its application as a fast primary on-bead screening instrument.

As demonstrated in Figure 4, autofluorescence levels of individual beads can vary significantly. Especially large libraries of heterocyclic scaffolds with a diverse set of aromatic building blocks often contain beads bearing fluorescent compounds or unwanted side products.

To demonstrate the power of our confocal detection technology for discriminating hit beads from autofluorescent beads under rather adverse conditions (i.e., within a library containing a significant number of autofluorescent beads), a library of heterocyclic AIDA tagged compounds[7] was incubated with Cy5-labeled target protein and scanned on PS02 (Figure 5). The scan image contains beads with intensity values spanning 2 orders of magnitude. Basically, four types of beads and intensity profiles are detectable: (a) dark beads with no bound target protein, (b) dark beads with significant target binding, (c) beads with increased autofluorescence and no protein binding, and (d) autofluorescent beads with an increased fluorescence signal on the surface due to protein binding.

Thus, while the reliable detection of hit beads is easily possible upon eye inspection from CONA scan images, a further prerequisite for an efficient screening system is the software based identification and automated quantification of beads throughout entire wells. For image evaluation, both

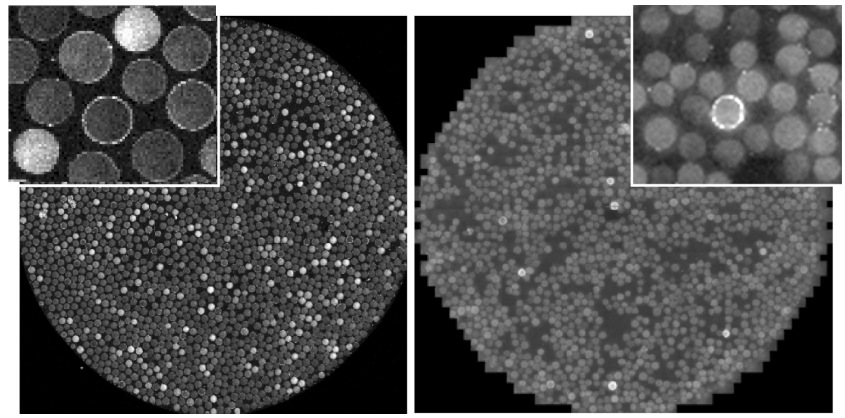

Figure 4. Typical single-well scan images acquired on the PS02 and PS04, respectively, and representative scan images of a monolayer of beads within a 96-well MTP. The beads, incubated with a Cy5-labeled target protein (50 nM) were imaged as described in the main text using the Cy5 excitation and emission filter sets (Table S1 of the Supporting Information). (left) PS02. (right) PS04. Zoomed sections of the wells are displayed in the inserts.

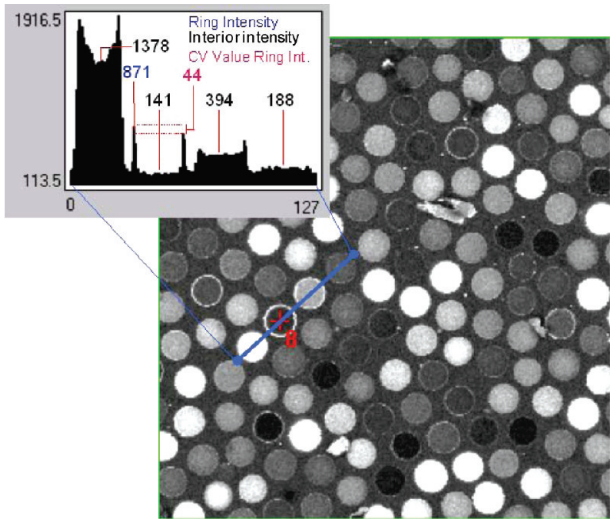

Figure 5. Bead intensity profiles in a typical CONA screen image. Zoom view of a CONA screening image of a MTP-well which contained a bead library with different levels of autofluorescence. A 1 mg portion of library beads were incubated with a Cy5-labeled target protein (50 nM). The scan was performed on PS02. The insert shows an intensity profile across four typical types of beads: a bead with a high level of autofluorescence (left), a hit bead with pronounced target protein binding and low autofluorescence, a hit bead with some target protein binding and a significant level of autofluorescence, and a dark bead with no target protein binding.

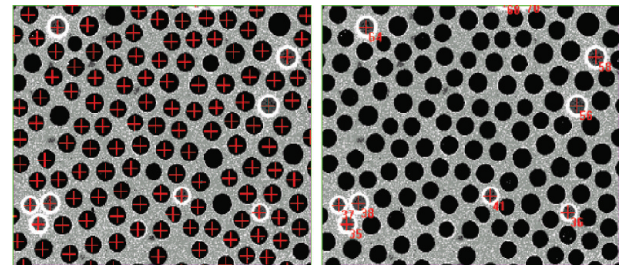

Figure 6. BeadEval software based bead detection. The BeadEval software procedure developed for the bead detection procedure starts with an image processing step (noise reduction, 5 × 5 pixel averaging, and logarithmic scaling and edge enhancement), followed by a Hough transformation based pattern recognition of beads. The center coordinates as well as the average ring intensity and interior intensity for each bead is calculated. Typical bead detection correctly identifies 90% of all beads, including the beads with the brightest fluorescence ring intensity (left image). Subsequently, a hit list of beads is generated, based on user defined parameters. The number assigned to each selected hit bead represents it's ranking in the pick-list (right image).

PS0X instruments use a Hough transformation algorithm, which requires manual threshold setting of parameters like bead size and combined variation (cv) value. In practice, optimal input parameters have to be determined for each screen and library. The bead detection algorithm, as implemented in PS02 and PS04 typically detects 90% of all beads within a well including those beads with the best fluorescent ring intensity (Figure 6). The remaining 10% of beads represent the darkest objects in a scanning image and therefore are irrelevant for hit bead detection. The automated bead detection procedure produces a bead list for all beads in each well of a MTP plate. Usually wells containing the highest ranked hit beads are selected for bead picking and rescanned immediately before picking. After rescanning, the well is reanalyzed, and the bead detection is used to select beads for picking. Following the resulting "picklist", the actual picking procedure is performed. The picking of a single bead requires approximately 180 s on PS02 and, due to a different picker arm stepping motor speed, 70 s on PS04.

During the bead picking process the hit bead, its surrounding neighbor beads, and the capillary tip can be monitored online via a dedicated video camera (Figure 1, bead monitor CCD). Figure 7 illustrates a successful picking event from the operator's perspective, i.e. seen through the bead monitor camera on PS02. The overall monolayer of the beads is not significantly affected by a single picking event. The beads in the immediate vicinity of a picked bead might move slightly due to the capillary suction process. However, as there are only a few hit beads contained in any one screening well, minor local bead displacements are irrelevant for the continued picking process. Thus, 20−30 beads can easily be picked from within one well of a 96-well MTP. If hit beads are located close to each other these wells can be quickly rescreened to cope with any bead repositioning. In general, the capillary based picking procedure proved to be very reliable with a success rate of ∼90%, and an average processivity of about 50 beads per day for PS02 and >100 beads for PS04 (if picked from multiple wells). The main reasons for delays during a bead picking session is due to

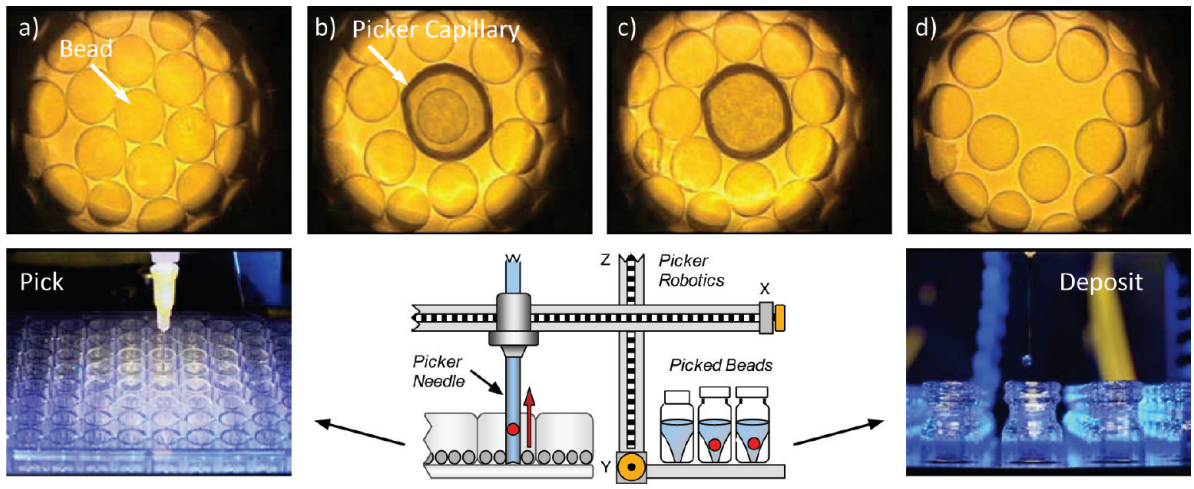

Figure 7. Bead picking. This image sequence illustrates the key steps of the bead isolation process. (a) Visualization of the hit bead (arrow) including its bead neighbors seen via the bright field imaging camera bead monitor. (b) Lowering the picker needle until the selected bead is fully engulfed by the capillary tip. (c) Extraction of the engulfed bead into the capillary—see empty capillary tube. (d) Remaining beads after retreating the capillary from the well. The two photographs at the bottom depict the picker needle before it is lowered into the well (left) and after the picking process before the picked bead is deposited into an MS-vial (right).

both "rescanning" of individual wells before picking and the need for regular system purging.

Discussion

To our knowledge, the described PS02 and PS04 instruments represent the first automated platform for on-bead screening of one-bead one-compound combinatorial libraries operated by confocal nanoscanning and bead picking. On the basis of a commercially available confocal fluorescence microscope chassis, both instruments have been designed to allow for large area confocal scanning and quantitative analysis of bead monolayers at the bottom of standard MTP formats. This large area scanning is achieved via a stepper-motor-driven *x*/*y* scanning stage for line scanning (PS02) and a Nipkow spinning disk for parallel recording of individual frames and tile image merging (PS04). The two methods for realizing a distortion free large area scanning of entire squared centimeter sized MTP wells lead to instruments with different application profiles. While both instruments clearly demonstrate the power of confocal detection methods in distinguishing between hit beads and autofluorescent beads, PS02 with its APD based detection is ideally suited for high resolution, quantitative analysis of small to medium sized libraries. PS04 on the other hand features an increased screening speed of up to 200 000 compounds in <7 h, however, at the expense of a slightly reduced image quality. The PS04's CCD-based detection and the tile image merging procedure, associated with the use of multiple parallel pinholes, are the main factors influencing the image quality on PS04.

Differences in solution and surface binding thermodynamics which often cause a problem in surface based screening methods can be overcome by a combination of physical and chemical methods. With the development of the PS02 and PS04 instruments, we addressed the necessity for high precision quantification of the fluorescently labeled target protein binding to a bead immobilized compound. The optical differentiation of the bead surface from the bead interior is essential for avoiding matrix connected optical artifacts and for staying closest to physiological buffer screening conditions. Therefore the confocal detection method is essential for ranking hit beads in on-bead screening. The intensity parameters derived from both APD and CDD detection methods allow efficient ranking of hit beads according to the amount of fluorescently labeled target protein bound to the immobilized compound.

It is also noteworthy that, in addition to on-bead screening, PS02 and PS04 are still used as "ordinary" confocal microscopes for fluorescence fluctuation analysis assays in MTP formats, using FCS, 2D-FIDA-anisotropy, 2-Color-2D-FIDA, FCCS, FIMDA, FILDA, cTRA, FRET, etc. as detection methods.

The only currently commercially available on-bead screening instrument, COPAS, operates based on a fluorescence activated bead sorting principle. In contrast, confocal nanoscanning on PS02 and PS04 provides an imaging based method for on-bead screening under true equilibrium conditions. Directly comparing PS04 with COPAS, both instruments achieve similar effective throughputs. However, the confocal scanning on the PS0X platform is fully automated, results in superior sensitivity, and allows for a reliable discrimination of autofluorescent beads and hit beads.

COPAS processes bead data "on the fly" and sorts hit beads based on predefined gate settings. Consequently, setting the bead intensity threshold level too low will result in a large number of sorted beads. It will then be necessary to rank a high number of hit beads after the sorting process is completed. As single hit beads are sorted into wells of many MTPs, physically locating the best ranked hits slows down the screening process. On the other hand, too stringent gate settings will lead to a loss of valuable hit beads.

In CONA, the actual screening process is independent from the bead picking process, all bead data can be analyzed before the top ranked hit beads are isolated. This avoids difficulties in threshold settings and allows for batchwise isolation of beads from one screening experiment. On COPAS, the sorting of hit beads is a "real-time triggered event", immediately following data recording. The accuracy of bead sorting can be as high as 95%; however, any failure leads to

an irreversible loss of hit beads. In contrast, the possibility for repetitive scanning and picking on the PS0X platform enables a "second, third, etc. chance" for isolating specific beads. Therefore the quick sublibrary based rescreening, picking, and data evaluation cycles on PS02 and PS04 instruments feature a process which we refer to as "science by screening" compared to the fully roboterized HTS generally performed in industry.

Furthermore, the ability to record traces of bead populations as a function of time, target concentration, additives, and many other parameters makes CONA ideally suited for mechanistic experiments, like measuring the kinetics of protein binding events and for on-bead competition assays.[7] Higher ligand−target affinities often encountered in on-bead binding provide an essential advantage in competition assays with low affinity reagents. Furthermore, experimental flaws, such as protein precipitation, autofluorescence, or "broken beads" are immediately detected in the scan images and only true hit beads are taken forward into subsequent characterization steps.

Abbreviations Used. PickoScreen instrument 02 or 04 (PS02, PS04, both PS0x); confocal nanoscanning, bead picking (CONA); microtiter plate (MTP); high throughput screening (HTS); complex objects and particle sorter (COPAS); polyethyleneglycole (PEG); fluorescence correlation spectroscopy (FCS); two-dimensional fluorescence intensity distribution analysis (2D-FIDA); fluorescence cross correlation spectroscopy (FCCS); fluorescence intensity multiple distribution analysis (FIMDA); fluorescence intensity lifetime distribution analysis (FILDA); confocal time-resolved anisotropy (cTRA); fluorescence resonance energy transfer (FRET).

Acknowledgment. The authors thank Dr. Timm Jessen for his long lasting support in developing the bead screening instruments. M.H. and C.B. contributed equally to this work.

Supporting Information Available. Description of PS02 standard components, filter settings and photographs of PS02 main components, photograph of the Nipkow based scanner and picker platform PS04, correlation between scan speed and resolution on PS02, and line scanning interruption. This material is available free of charge via the Internet at http://pubs.acs.org.

References and Notes

(1) Diller, D. J.; Hobbs, D. W. *J. Med. Chem.* **2004**, *47* (25), 6373–6383.
(2) Alanine, A.; Nettekoven, M.; Roberts, E.; Thomas, A. W. *Comb. Chem. High Throughput Screen.* **2003**, *6* (1), 51–66.
(3) Davies, J. W.; Glick, M.; Jenkins, J. L. *Curr. Opin. Chem. Biol.* **2006**, *10* (4), 343–351.
(4) Kodadek, T.; Bachhawat-Sikder, K. *Molec. Biosyst.* **2006**, *2* (1), 25–35.
(5) Lam, K. S.; Salmon, S. E.; Hersh, E. M.; Hruby, V. J.; Kazmierski, W. M.; Knapp, R. J. *Nature* **1991**, *354* (6348), 82–84.
(6) Meisner, N. C.; Hintersteiner, M.; Uhl, V.; Weidemann, T.; Schmied, M.; Gstach, H.; Auer, M. *Curr. Opin. Chem. Biol.* **2004**, *8* (4), 424–431.
(7) Meisner, N.-C.; Hintersteiner, M.; Seifert, J.-M.; Bauer, R.; Benoit Roger, M.; Widmer, A.; Schindler, T.; Uhl, V.; Lang, M.; Gstach, H.; Auer, M. *J. Mol. Biol.* **2009**, *386* (2), 435–50.
(8) Lim, H.-S.; Archer, C. T.; Kodadek, T. *J. Am. Chem. Soc.* **2007**, *129* (25), 7750–7751.
(9) Park, S.-H.; Wang, X.; Liu, R.; Lam, K. S.; Weiss, R. H. *Cancer Biol. Ther.* **2008**, *7* (12), 2015–2022.
(10) Zhang, Y.; Zhou, S.; Wavreille, A.-S.; DeWille, J.; Pei, D. *J. Comb. Chem.* **2008**, *10* (2), 247–255.
(11) Chen, X.; Tan, P. H.; Zhang, Y.; Pei, D. *J. Comb. Chem.* **2009**, *11* (4), 604−611.
(12) Lam, K. S.; Lebl, M.; Krchnak, V. *Chem. Rev.* **1997**, *97* (2), 411–448.
(13) Olivos, H. J.; Bachhawat-Sikder, K.; Kodadek, T. *Chembiochem* **2003**, *4* (11), 1242–1245.
(14) Sweeney, M. C.; Wavreille, A. S.; Park, J.; Butchar, J. P.; Tridandapani, S.; Pei, D. *Biochemistry* **2005**, *44* (45), 14932–14947.
(15) Lehman, A.; Gholami, S.; Hahn, M.; Lam, K. S. *J. Comb. Chem.* **2006**, *8* (4), 562–570.
(16) Mueller, K.; Gombert, F. O.; Manning, U.; Grossmueller, F.; Graff, P.; Zaegel, h.; Zuber, j. F.; Freuler, F.; Tschopp, C.; Baumann, G. *J. Biol. Chem.* **1996**, *271* (28), 16500–16505.
(17) Youngquist, R. S.; Fuentes, G. R.; Lacey, M. P.; Keough, T. *J. Am. Chem. Soc.* **1995**, *117* (14), 3900–3906.
(18) Wang, X.; Peng, L.; Liu, R.; Xu, B.; Lam, K. S. *J. Pept. Res.* **2005**, *65* (1), 130–138.
(19) Hintersteiner, M.; Auer, M. *Ann. N.Y. Acad. Sci.* **2008**, *1130*, 1–11.
(20) Wang, P.; Arabaci, G.; Pei, D. *J. Comb. Chem.* **2001**, *3* (3), 251–254.
(21) Boeijen, A.; Liskamp, R. M. J. *Tetrahedron Lett.* **1998**, *39* (21), 3589–3592.
(22) Ding, H.; Prodinger, W. M.; Kopecek, J. *Biomacromolecules* **2006**, *7* (11), 3037–3046.
(23) Marani, M. M.; Martinez Ceron, M. C.; Giudicessi, S. L.; de Oliveira, E.; Cote, S.; Erra-Balsells, R.; Albericio, F.; Cascone, O.; Camperi, S. A. *J. Comb. Chem.* **2009**, *11* (1), 146–150.
(24) Meldal, M. *Biopolymers* **2002**, *66* (2), 93–100.
(25) Reddy, M. M.; Bachhawat-Sikder, K.; Kodadek, T. *Chem. Biol.* **2004**, *11* (8), 1127–1137.
(26) Hiemstra, H. S.; Benckhuijsen, W. E.; Amons, R.; Rapp, W.; Drijfhout, J. W. *J. Pept. Sci.* **1998**, *4* (4), 282–288.
(27) Davies, E. R. *Machine Vision*, 2nd ed.; Academic Press: New York, 1997.
(28) Ballard, D. H. *Pattern Recognition* **1981**, *13* (2), 111–122.
(29) Nipkow, P. G. *Elektrisches Teleskop*, **1884**.
(30) Nakano, A. *Cell Struct. Funct.* **2002**, *27* (5), 349–355.
(31) Inoue, S.; Inoue, T. *Methods Cell Biol.* **2002**, *70*, 87–127.
(32) Pawley, J. B. *Handbook of Biological Confocal Microscopy*; 2nd ed.; Plenum Press: New York, 1995.

CC900059Q